Cr:ZnSe laser incorporating anti-reflection microstructures exhibiting low-loss, damage-resistant lasing at near quantum limit efficiency

Sean McDaniel,[1,*] Douglas Hobbs,[2] Bruce MacLeod,[2] Ernest Sabatino,[2] Patrick Berry,[3] Kenneth Schepler,[4] William Mitchell,[3] and Gary Cook[3]

[1]Leidos Inc., 3745 Pentagon Blvd, Beavercreek, OH, 45431, USA
[2]TelAztec LLC, 15 A Street, Burlington, MA 01803,USA
[3]U.S. Air Force Research Laboratory, 2241 Avionics Circle, Wright-Patterson AFB, OH, 45433, USA
[4]CREOL, The College of Optics & Photonics, University of Central Florida, Orlando, FL, 32816, USA
[*]sean.a.mcdaniel@leidos.com

Abstract: We report demonstration of efficient continuous-wave lasing from chromium-doped zinc selenide using anti-reflection microstructures (ARMs) in place of thin-film AR coatings or Brewster angle cavity geometries. ARM textures are more resistant to laser-induced damage than coatings, exhibit low-loss, wide angular acceptance, broad wavelength effectiveness, and are not susceptible to water absorption. Slope-efficiencies of 68% were achieved, which compares favorably to the thin-film control samples at 58% for the same cavity. ARMs hold promise for near-term power scaling and wavelength agility of transition-metal-ion doped II-VI lasers.

OCIS codes: (310.1210) Antireflection coatings; (310.6628) Subwavelength structures, nanostructures; (140.3580) Lasers, solid-state.

References and links

1. S. Mirov, V. Fedorov, I. Moskalev, M. Mirov, and D. Martyshkin, "Frontiers of mid-infrared lasers based on transition metal doped II–VI semiconductors," J. Lumin. **133**, 268–275 (2013).
2. P. A. Berry and K. L. Schepler, "High-power, widely-tunable Cr^{2+}:ZnSe master oscillator power amplifier systems," Opt. Express **18**(14), 15062–15072 (2010).
3. K. T. Zawilski, S. D. Setzler, P. G. Schunemann, and T. M. Pollak, "Laser damage threshold of single crystal $ZnGeP_2$ at 2.05 μm," Proc. SPIE **5991**, 599104 (2005).
4. H. Krol, C. Grèzes-Besset, L. Gallais, J. Natoli, and M. Commandré, "Study of laser-induced damage at 2 microns on coated and uncoated ZnSe substrates," Proc. SPIE **6403**, 640316 (2006).
5. B. D. MacLeod, D. S. Hobbs, and E. Sabatino III, "Moldable AR microstructures for improved laser transmission and damage resistance in CIRCM fiber optic beam delivery systems," Proc. SPIE **8016**, 80160Q (2011).
6. D. S. Hobbs, B. D. MacLeod, E. Sabatino III, S. B. Mirov, and D. V. Martyshkin, "Laser damage resistant anti-reflection microstructures for mid-infrared metal-ion doped ZnSe gain media," Proc. SPIE 8530, 85300P (2012).
7. S. J. Wilson and M. C. Hutley, "The optical properties of 'moth eye' antireflection surfaces," Opt. Acta (Lond.) **29**(7), 993–1009 (1982).
8. D. S. Hobbs and B. D. MacLeod, "Design, fabrication and measured performance of anti-reflecting surface textures in infrared transmitting materials," Proc. SPIE **5786**, 349–364 (2005).
9. D. Findlay and R. A. Clay, "The measurement of internal losses in 4-level lasers," Phys. Lett. **20**(3), 277–278 (1966).
10. J. Caird, S. Payne, P. Staver, A. Ramponi, L. Chase, and W. Krupke, "Quantum Electronics Properties of the NaGaLiF: Cr3+," IEEE J. Quantum Electron. **QE-24**, 1077 (1988).

1. Introduction

The nature of absorption by organic and other chemicals in the atmosphere and human body drives development of lasers able to operate in the middle-infrared (mid-IR) wavelength region, particularly the 2-5 μm range. Mid-IR lasers being developed for medical, scientific and military applications must operate with wide-band tunability, versatility and high average

#220993 - $15.00 USD Received 15 Aug 2014; revised 24 Sep 2014; accepted 26 Sep 2014; published 2 Oct 2014

power output in both continuous wave (CW) and pulsed configurations. Military platforms additionally require compact, light-weight, high efficiency lasers that are robust and long-lived.

One family of solid-state lasers which has shown promising mid-IR performance is that of the transition-metal-ion doped II-VI materials. Crystals of zinc sulfide (ZnS), zinc selenide (ZnSe), and zinc telluride (ZnTe) diffusion doped with chromium (Cr^{2+}), cobalt (Co^{2+}), iron (Fe^{2+}), or nickel (Ni^{2+}) ions, have been demonstrated with Cr:ZnSe and Cr:ZnS making the most progress in all operational modes (CW, gain-switched high average power, gain-switched high pulse energy and modelocked) [1]. Even these lasers however, have been limited in power scaling by thermal quenching, damage, and delamination issues due to water adsorption commonly present with mid-IR anti-reflection (AR) coatings.

Efficient laser operation and power scaling requires the elimination of reflection losses from the facets of the crystal gain media. Pumping a gain crystal facet cut at Brewster's angle is one method for eliminating back reflections, but this configuration requires the use of polarized pump light and complex, astigmatically-compensated cavity designs. An alternative is to deposit thin-film AR multi-layer coatings (TFARCs) on the crystal facets, but these coatings perform over a limited bandwidth and introduce additional material problems such as absorption, defects, and degradation over time. These factors lead to a general decrease in the crystal's damage resistance. For example, as seen in Fig. 1 below, power scaling work on the oscillator portion of a 14 W master oscillator/power amplifier [2] produced damage to the AR coating, the surface and the sub-surface of the Cr:ZnSe crystal at pump levels of 10-40 W at 1908 nm and beam diameters of 100-400 μm (0.1 to 12 kW/cm^2). Pulsed laser damage thresholds for TFARC stacks are also quite low, often reported in the 0.5 to 2.0 J/cm^2 range for the mid-IR wavelength of 2.1 μm, a level two to five times lower than the uncoated base material surface [3–6].

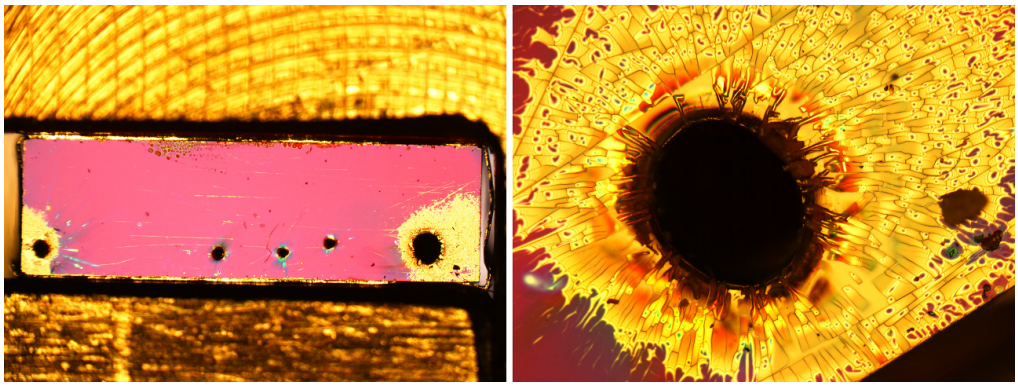

Fig. 1. Coating and surface damage (left) to the 6.5 mm x 1.8 mm face of a Cr:ZnSe sample under CW pumping and a close-up (right) of the largest (~400 μm diameter) damage spot.

A new approach, which avoids these problems, is to etch an array of surface relief microstructures into the facets of the laser gain media. When the size and spacing of the features of these textures are much smaller than the laser wavelength, a graded refractive index is created which allows light to propagate through the crystal facet without losses due to reflection, diffraction or scattering. Often referred to as "Motheye" textures in the literature [3,4], a typical design involves an array of cone-like protrusions. Such AR microstructures (ARMs) can provide a robust, single material solution for wide bandwidth use and the high laser damage resistance required for further power scaling. The end goal for these designs is to achieve a laser-induced damage threshold (LiDT) that can match or exceed the level of a well-polished surface; a survivability many times higher than an equivalent performance broad-band TFARC.

#220993 - $15.00 USD Received 15 Aug 2014; revised 24 Sep 2014; accepted 26 Sep 2014; published 2 Oct 2014

In this paper, we demonstrate operation of a Cr:ZnSe laser using ARMs. The ARM treated sample exhibited low-loss performance when utilized in a laser cavity. The losses due to the ARM treated sample were directly compared to a thin-film AR coated sample in the same laser resonator. Finally, the laser was tuned over a 300 nm range to demonstrate broad wavelength operation of the laser.

2. Anti-reflection microstructures

To obtain the benefits of ARM technology for mid-IR lasers, the AR surface relief structure was etched directly into the laser gain medium. By removing material rather than adding dissimilar materials, which is the basis for thin-film AR coatings, the ARM solution for Cr:ZnSe lasers does not suffer from film limitations of absorption and thermal stresses leading to delamination and degraded damage resistance [5–7].

The fabrication process for ARMs in Cr:ZnSe is illustrated in Fig. 2. The process begins with coating the Cr:ZnSe laser crystal facets with a conventional photoresist (Step 1). Next, a non-contact, maskless lithography technique is employed to expose a latent image of the AR texture in the photoresist layer (Step 2). The lithography was completed (Step 3) with a wet development that reduced the photoresist to a uniform periodic array of pillars. These pillars serve as a mask during a reactive ion etch (Step 4) process that transfers the photoresist image into the Cr:ZnSe laser crystal facet. A final stage cleaning process (Step 5), removes any residual photoresist or contaminants from the etch plasma.

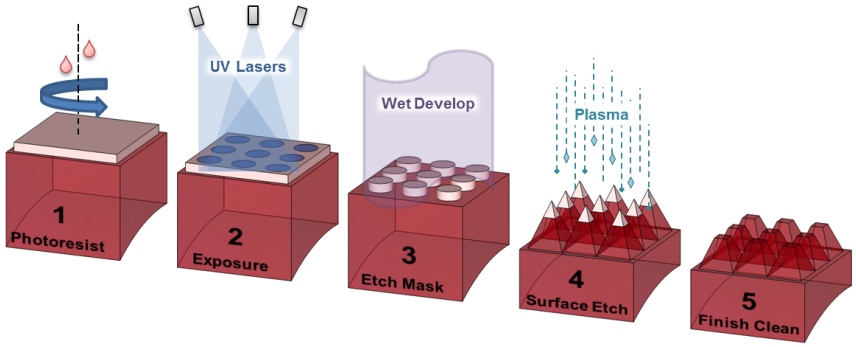

Fig. 2. Process flow for fabricating AR microstructures in Cr:ZnSe laser crystals.

A typical size of a tunable Cr:ZnSe laser crystal for mid-IR applications is on the order of 9 mm x 3 mm x 5 mm (L x W x H), where the 3 mm x 5 mm facets require an AR treatment. The inherent durability of ARM textures etched in Cr:ZnSe lends itself to applications requiring large area discs. Additionally, these discs are convenient for the lithography and etch processes described in Fig. 2. Cleaning of the ARM textures is readily accomplished with solvent rinsing or the drag-and drop methods typically employed for cleaning TFARCs. Because there are no additional material layers that can degrade or lose adhesion, ARM textures can be more aggressively cleaned than TFARCs. Immersion in a heated ammonia solution with ultrasonic agitation has been used for ARM treated Cr:ZnSe, as well as isotropic oxygen plasma cleaning.

The feature height and spacing within the periodic structure of ARMs is configured to be much smaller than any operational wavelength to preclude any losses due to scattering or diffraction. The pitch of the honeycomb array of cones was set to 740 nm, which for on-axis illumination would produce free-space propagating first order diffracted beams at wavelengths less than the pattern pitch times the material refractive index, 740 nm x 2.44 = 1805 nm in this case, a wavelength well below the pump and tuning bands of Cr:ZnSe gain material. Micrographs, showing the array of 1200 nm high cones that make up a typical

#220993 - $15.00 USD Received 15 Aug 2014; revised 24 Sep 2014; accepted 26 Sep 2014; published 2 Oct 2014

Motheye ARM texture, are shown by the scanning electron microscope (SEM) images in Fig. 3.

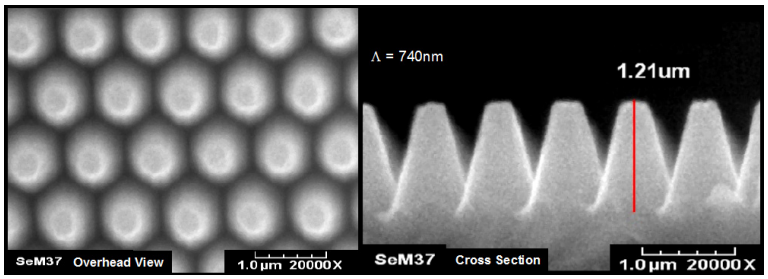

Fig. 3. Overhead (left) and cross sectional (right) views of an ARM-treated Cr:ZnSe laser crystal.

The measured spectral transmission of an ARM treated Cr:ZnSe laser crystal is shown as the solid black curve in Fig. 4. Accounting for the chromium absorption loss, Fresnel reflection losses over the wavelength range of 1.9-3.1 µm, were reduced below 3%. Peak transmission was measured to be greater than 99.7% at 2.5 µm. For comparison, the transmission of an untreated (no AR treatment) Cr:ZnSe crystal and a TFARC treated Cr:ZnSe crystal are shown as the dashed dark grey and light grey curves, respectively. The TFARC was done by a commercial vendor and consisted of a 5 layer stack of proprietary material composition. All three 15 mm diameter Cr:ZnSe crystals are pictured in the inset. The transmission of the TFARC sample is less than the ARM treated sample and experiences water absorption in the wavelength range from 2.7 to 3.4 µm. However, it should be noted that not all coatings exhibit water absorption in the 2.7-3.4 µm range and the spectral response of TFARCs is highly dependent on the type of material and process used for production of the thin-film stack. Additionally, the ARM transmission decreases gradually and monotonically past 3.4 µm while the TFARC transmission shows greater loss and spectral variation. It should be noted that all three Cr:ZnSe discs displayed in Fig. 4 were doped to the same Cr^{2+} level by IPG Photonics. The additional loss below 1.8 µm wavelength for the ARM disc is due to free space diffraction from the ARM surface texture. The transmission minimum at 1.8 µm for the TFARC disc is slightly higher than the untreated disc due to the effects of the thin film coating. This highlights the major advantages for ARM textures incorporated into mid-IR laser systems operating in this water absorption band, namely higher broadband transmission and an increased resistance to pulsed laser induced damage compared to TFARCs [8].

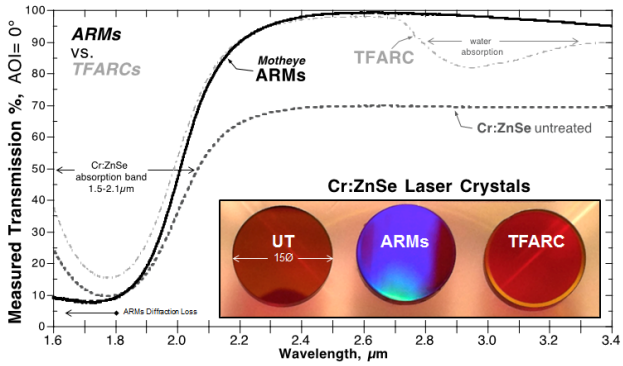

Fig. 4. Measured transmission of ARM treated sample compared to a traditional thin-film AR coated sample (TFARC) and untreated (UT) sample. The AR treatment design band is continuous from the pump laser at 1.9µm out to the longest tuning wavelength at 3.2µm. The three discs displayed in the lower right-hand corner were 15 mm diameter samples.

#220993 - $15.00 USD Received 15 Aug 2014; revised 24 Sep 2014; accepted 26 Sep 2014; published 2 Oct 2014

3. Experimental setup

The experimental setup, shown in Fig. 5, consisted of an ARM textured Cr:ZnSe crystal mounted in a direct water impingement heat sink, shown in Fig. 6, with the cross sectional diagram. The heat sink design permitted direct contact of flowing water with the crystal to increase thermal handling of the system. The Cr:ZnSe crystal was a 3.58 mm thick disk, diameter of 1.5 cm, doped with Cr^{2+} ions to a concentrationof $6x10^{18}$ ions/cm^3. A second crystal with identical dimensions, doping level, and polish was coated with a traditional thin-film AR stack. Both crystals were supplied by IPG Photonics. The 1.9 µm emission from an IPG Photonics TLR-LP 20 W thulium fiber laser was focused into the cavity using a 7.5 cm focal length lens, *L1*. The beam was focused to a $1/e^2$ spot size of 65 µm inside of the crystal. Cavity mirror *M1* was a 5 cm radius of curvature (ROC) mirror which was AR coated for 1.9 µm and HR coated for 2-3 µm. Mirror *M2* was a 10 cm ROC folding mirror AR coated for 1.9 µm and HR coated for 2.3-3 µm. *M3* was a variable percentage outcoupler for 2.3-3 µm. Additionally, the optics *TP1* and *M4* were used to demonstrate tuning of the laser. *TP1* was an uncoated CaF_2 prism and *M4* was a 90% reflective outcoupler for 2.3-3 µm.

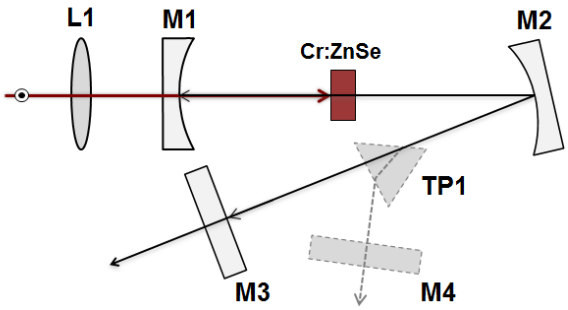

Fig. 5. Experimental setup to directly compare ARMs and TFARC crystals.

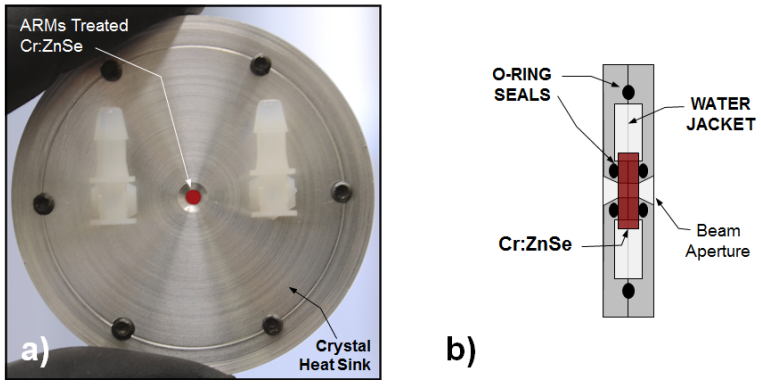

Fig. 6. a) Heat sink used to direct water impingement cool the ARM textured Cr:ZnSe disk . b) Cross-section of the direct water impingement heat sink.

4. Experimental results

The laser resonator described above was characterized with both ARM treated and TFARC samples. Three outcouplers were tested in order to better characterize the passive losses of the cavity. Both samples, ARM and thin-film, were tested using each outcoupler up to an approximate pump power of 4 W (Fig. 7). The tabulated slope efficiencies for the ARMs and TFARC samples can be seen in Table 1. A comparison of the slope efficiencies for each sample demonstrated the ARM treated sample performed better than the TFARC sample. For

#220993 - $15.00 USD Received 15 Aug 2014; revised 24 Sep 2014; accepted 26 Sep 2014; published 2 Oct 2014

the best performing outcoupler, 70% reflective, the slope efficiency was 16% higher for the ARM sample than for the thin-film sample. It should be noted that these slope efficiencies were fitted neglecting data points near threshold.

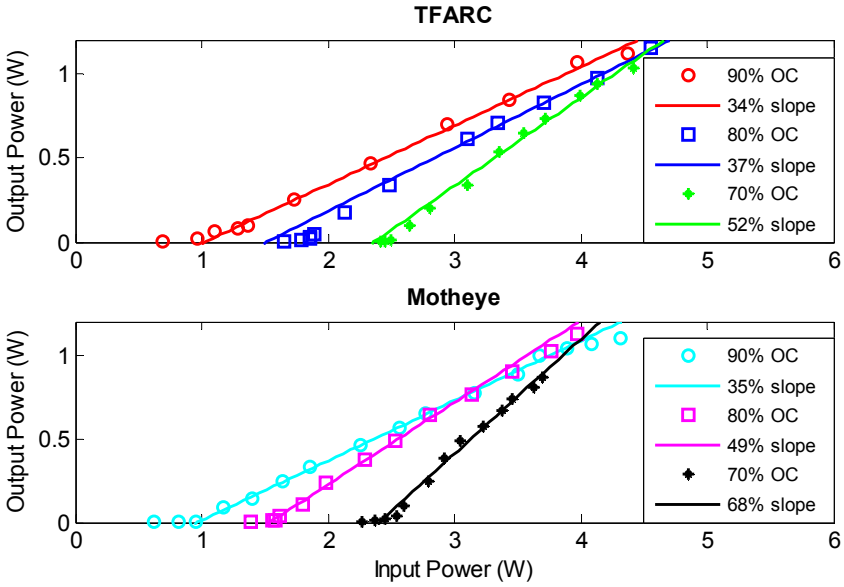

Fig. 7. Measured slope efficiencies of the ARM textured ("Motheye") and TFARC samples in identical resonators.

Table 1. Comparison of slope efficiencies for thin-film AR coated samples and ARM coated samples.

Outcoupler	ARM	TFARC
70%	68%	52%
80%	49%	37%
90%	35%	34%

The slope efficiency measurements do not provide sufficient information to directly compare the two AR treatment methods. In order to relate passive losses from the cavity, a Findlay-Clay analysis [9] was performed for the system. The Findlay-Clay analysis, Fig. 8, shows the round-trip passive losses for the ARM treated sample were significantly lower than the thin-film coated sample, yielding values of 0.5% for the ARM textured sample and 1.7% for the TFARC sample. Thus, the ARM textured samples have lower passive losses and lower threshold as compared to the regular AR coating. Threshold lasing was observed using an extended range InGaAs detector, which had a noise equivalent power of 2 pW/√Hz. As soon as lasing was observed with the detector, the corresponding input power was recorded. This method of measuring the laser threshold avoids errors from extrapolated slope efficiency determinations of the lasing threshold and improves the accuracy of Findlay-Clay analysis for laser materials with poor thermal conductivity. Owing to the influence of thermal lensing on the slope efficiency of the laser at pump powers much higher than the threshold values, the alternative method of Caird analysis [10] was not performed here to determine the resonator losses.

#220993 - $15.00 USD Received 15 Aug 2014; revised 24 Sep 2014; accepted 26 Sep 2014; published 2 Oct 2014

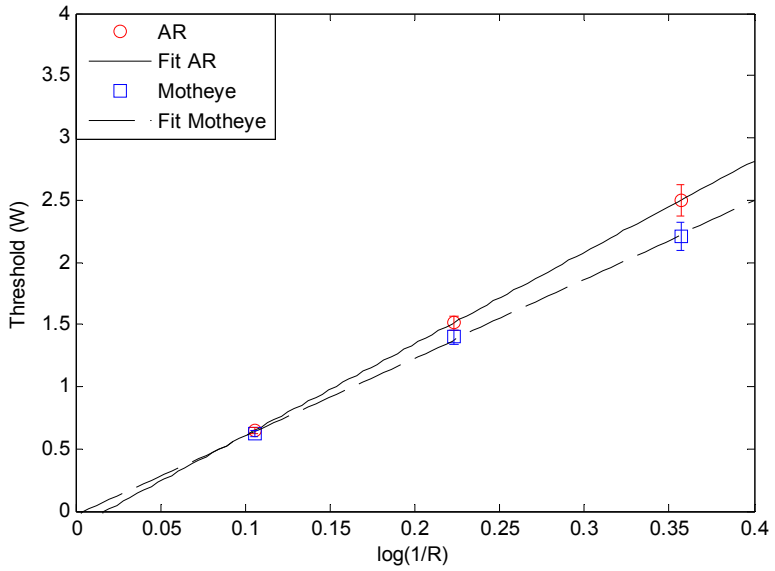

Fig. 8. Findlay-Clay analysis for the ARMs-textured and TFARC Cr:ZnSe samples.

The laser was tuned to evaluate the wavelength performance of the intracavity elements. Laser tuning was effected using a CaF_2 prism with a 90% reflective outcoupler. Tuning was achieved by slight rotation to the outcoupler to provide feedback from a different wavelength due to the dispersion of the prism. Figure 9 illustrates the tuning range of the ARM textured sample. The free-running center wavelength was observed to be centered at 2389 nm. A similar tuning curve was obtained for the TFARC sample. The relatively narrow tuning spectrum (2289 nm – 2538 nm) was likely due to the use of a non-optimized uncoated tuning prism.

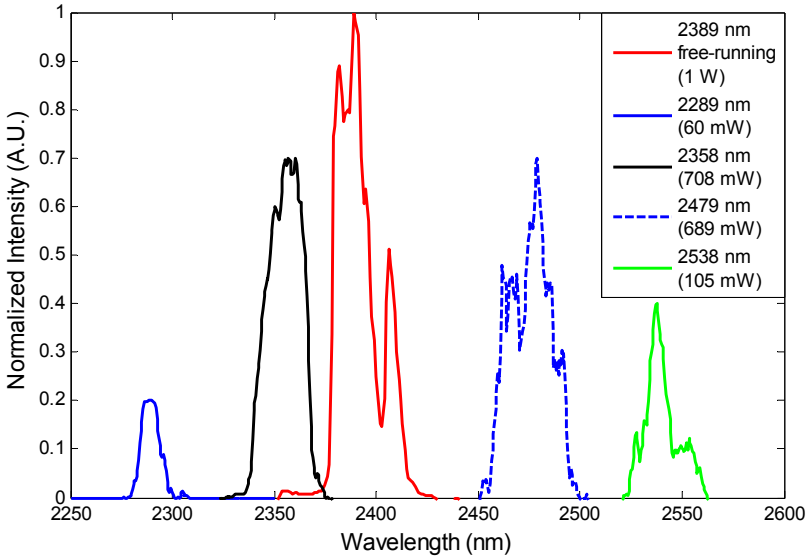

Fig. 9. Discrete tuning spectra of the ARM treated sample. The free-running wavelength was centered at 2389 nm.

#220993 - $15.00 USD Received 15 Aug 2014; revised 24 Sep 2014; accepted 26 Sep 2014; published 2 Oct 2014

5. Conclusion

In conclusion, we have demonstrated operation of a Cr:ZnSe laser utilizing graded-index anti-reflection microstructures in place of conventional thin-film AR coatings. The laser achieved 1.1 W of output at 4.1 W of input power yielding a slope efficiency of 68%. The achieved slope efficiency was approximately 11% lower than the theoretical quantum limited slope efficiency of 79% for the center emission wavelength. Comparing passive losses from a thin-film AR coated sample to the passive losses of an ARM treated sample revealed that the ARM treated sample had resonator losses that were 1.2% lower than the thin-film coated sample. ARM texturing has great promise as a rugged AR surface suitable for high power mid-IR laser optical devices.

#220993 - $15.00 USD Received 15 Aug 2014; revised 24 Sep 2014; accepted 26 Sep 2014; published 2 Oct 2014